International Journal of Heat and Mass Transfer 82 (2015) 123–134

Contents lists available at ScienceDirect

International Journal of Heat and Mass Transfer

journal homepage: www.elsevier.com/locate/ijhmt

On the influence of gravitational and centrifugal buoyancy on laminar flow and heat transfer in curved pipes and coils

Michele Ciofalo *, Antonino Arini, Massimiliano Di Liberto

Dipartimento Energia, Ingegneria dell'Informazione e Modelli Matematici (DEIM), Università di Palermo, Viale delle Scienze, I-90128 Palermo, Italy

ARTICLE INFO

Article history:
Received 11 July 2014
Received in revised form 31 October 2014
Accepted 31 October 2014

Keywords:
Curved pipe
Helical coil
Gravitational buoyancy
Centrifugal buoyancy
Computational fluid dynamics
Laminar flow
Heat transfer

ABSTRACT

The effects of gravitational and centrifugal buoyancy on laminar flow and heat transfer in curved and helical pipes were investigated by numerical simulation. Six dimensionless numbers characterizing the problem were identified, and an analysis was conducted on the possible combinations of signs of the gravitational and centrifugal buoyancy effects. Two distinct Richardson numbers were introduced in order to quantify the importance of the two types of buoyancy, and it was shown that, in the case of heating from the wall, a maximum realizable value of the centrifugal Richardson number exists which is a linear function of the curvature δ (ratio of pipe radius a to curvature radius c). Detailed results were obtained for $\delta = 0.9$, torsion λ (ratio of reduced pitch $H/(2\pi)$ to curvature radius c) = 0 (toroidal pipe) or 0.4 (helical pipe), Re = 100, Pr = 1 and gravitational and centrifugal Richardson numbers Ri_g, Ri_c each varying from −0.1 to +0.1. A complex interaction between the two forms of buoyancy was found to exist. In the helical geometry, provided $|\mathrm{Ri}_g| \approx |\mathrm{Ri}_c|$ they exhibited effects of the same order. The lowest values of both the friction coefficient and the mean Nusselt number were obtained in the presence of positive gravitational and centrifugal buoyancy, while the highest values were obtained when both forms of buoyancy were negative; the reason for this behavior was identified in the different degree of coupling between the distributions of axial velocity and temperature. In the toroidal geometry, a simpler behavior was predicted due to the presence of top–bottom symmetry; both the friction coefficient and the mean Nusselt number were found to decrease with the intensity of centrifugal buoyancy and to be little affected by gravitational buoyancy in the range of Ri_g investigated.

1. Problem definition

Helical coils are widely used in heat exchangers and steam generators, both because they easily accommodate thermal expansion and because they may exhibit higher heat transfer rates than straight pipes [1,2]. Fig. 1 shows a schematic representation of a single turn of a helical coil with its characteristic geometrical parameters: coil radius c, pipe radius a, and coil pitch $2\pi b$.

Several studies, e.g. [3–5], show that coil torsion $\lambda = b/c$ has only a higher order effect on the flow and on global quantities, such as the friction coefficient, with respect to the first order effect of curvature $\delta = a/c$.

When $\lambda = 0$, a helical coil is reduced to a curved pipe whose axis lies in a plane. Such a constant-curvature planar pipe can only be a closed torus or a toroidal segment. The former has little practical application because of the obvious difficulty of maintaining a permanent motion of the fluid, but can be of considerable theoretical interest and has been the subject of several studies, especially regarding the inception and characteristics of turbulence [6–11]. On the contrary, the latter is of great practical importance, e.g. in the prediction of singular pressure losses in bends, fittings and serpentine pipes, but cannot exhibit fully developed flow and heat transfer and therefore will not be considered in the present study.

2. Flow and heat transfer in curved pipes and coils

2.1. Flow field and pressure drop

Flow in curved pipes with zero torsion is characterized by the existence of a top–bottom symmetric secondary circulation in the cross section, caused by the local imbalance between pressure and inertial (centrifugal) forces. The fluid moves towards the outer bend side near the equatorial midplane, returns towards the inner side along two near-wall boundary layers, and then forms two symmetric secondary cells (Dean vortices) having a characteristic velocity scale $U\delta^{1/2}$. Fig. 2(a) shows such a secondary flow pattern

* Corresponding author.
E-mail address: michele.ciofalo@unipa.it (M. Ciofalo).

http://dx.doi.org/10.1016/j.ijheatmasstransfer.2014.10.074
0017-9310/

Nomenclature

a	pipe radius [m]
b	reduced pitch, $H/(2\pi)$ [m]
c	curvature radius [m]
c_p	specific heat [J kg^{-1} K^{-1}]
d	pipe diameter, $2a$ [m]
De	Dean number, $\mathrm{Re}\sqrt{\delta}$
f	Darcy friction coefficient
Gr_c	centrifugal Grashof number, Eq. (6)
Gr_g	gravitational Grashof number, Eq. (5)
g_z	vertical component of gravity acceleration [m s^{-2}]
N	number of control volumes in grid
k	thermal conductivity [W m^{-1} K^{-1}]
Nu	mean Nusselt number, $d\langle q''_w\rangle/[k(T_w - T_b)]$
Pr	Prandtl number, $c_p\mu/k$
p	pressure [Pa]
$\mathbf{p}_s$	opposite of streamwise pressure gradient [Pa m^{-1}]
q''	heat flux [W m^{-2}]
r	local radius of curvature [m]
Re	bulk Reynolds number, $Ud\rho_b/\mu_b$
Re_τ	friction velocity Reynolds number, $u_\tau a\rho_b/\mu_b$
Ri_c	centrifugal Richardson number, Eq. (9)
Ri_g	gravitational Richardson number, Eq. (8)
s	curvilinear abscissa along the pipe axis [m]
S	heat source term [W m^{-3}]
t	time [s]
T	temperature [K]
U	density-averaged fluid velocity [m s^{-1}]
u_i	ith velocity component [m s^{-1}]
u_τ	friction velocity, $\sqrt{\langle\tau_w\rangle/\rho_b}$ [m s^{-1}]
x, y, z	Cartesian coordinates [m]

Greek symbols

β	volumetric expansion coefficient, $-(1/\rho_0)\partial\rho/\partial T$ [K^{-1}]
δ	dimensionless curvature, a/c
Δt	time step [s]
λ	dimensionless torsion, b/c
μ	viscosity [kg m^{-1} s^{-1}]
ν	kinematic viscosity, μ/ρ [m^2 s^{-1}]
ρ	density [kg m^{-3}]
τ_w	wall shear stress [Nm^{-2}]

Subscripts

b	bulk
RAD	radial
s	streamwise (axial) direction
w	wall
θ	azimuthal direction
z	vertical direction

Averages

$\langle\cdot\rangle$	wall-averaged

for Re = 100 and a very high curvature ($\delta = 0.9$); the corresponding toroidal geometry is shown in Fig. 2(c). This picture changes for finite values of the torsion, which breaks the top–bottom symmetry of the secondary flow; Fig. 2(b) reports the secondary flow pattern for the same Re and δ as Fig. 2(a), but a torsion $\lambda = 0.4$; the corresponding helical geometry is shown in Fig. 2(d). It can be seen that (assuming the fluid to flow upwards in the coil) torsion reinforces the lower recirculation cell while weakening the upper one.

Experimental pressure drop results for a wide range of curvatures and Reynolds numbers were presented by Ito [12], who derived the following correlations for the Darcy–Weisbach friction factor f (four times the Fanning coefficient) in curved pipes ($5\times10^{-4} \leqslant \delta \leqslant 0.2$):

$$f = \frac{64}{\mathrm{Re}}\cdot\frac{21.5\cdot\mathrm{De}}{(1.56+\log_{10}\mathrm{De})^{5.73}} \qquad \text{(laminar flow)} \tag{1}$$

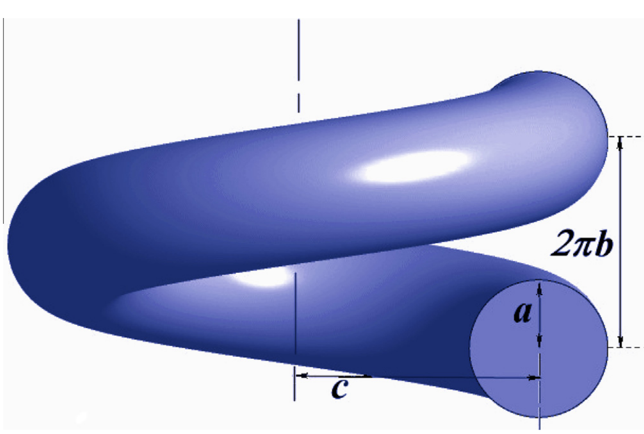

Fig. 1. Schematic representation of a helically coiled pipe with its main geometrical parameters: a, pipe radius; c, coil radius; $2\pi b$, coil pitch. Only one coil turn is shown (computational domain).

$$f = 0.304\cdot\mathrm{Re}^{-0.25} + 0.029\sqrt{\delta} \qquad \text{(turbulent flow)} \tag{2}$$

The Dean number $\mathrm{De} = \mathrm{Re}\sqrt{\delta}$ accounts for inertial, centrifugal and viscous effects. Note that Eqs. (1) and (2) do not explicitly contain torsion.

Ito's correlations have been confirmed to a notable degree by a large bulk of experimental studies; for example, they agree well with the experiments conducted by Cioncolini and Santini [13] in a broad range of curvatures ($0.027 \leqslant \delta \leqslant 0.143$) and Reynolds numbers ($\mathrm{Re} \approx 10^3$–$7\times10^4$).

2.2. Heat transfer

As regards heat transfer, many experimental studies were performed in the 1960s and the 1970s on the average heat transfer rate in curved and helical pipes [14–16]. Only some of these investigations explored the influence of the Prandtl number on heat transfer, and very few investigated the local heat transfer rate distribution.

More recently, Xin and Ebadian [17] presented an experimental study of heat transfer in helical pipes; the authors explored two values of curvature, i.e. $\delta = 0.027$ and 0.08, Re from 5×10^3 to 1.1×10^5, and three different fluids, i.e. air (Pr = 0.7), water (Pr = 5), and ethylene glycol (Pr = 175), covering a broad range of Prandtl numbers. Results were approximated by the following correlations:

$$\mathrm{Nu} = (2.153 + 0.318\,\mathrm{De}^{0.643})\mathrm{Pr}^{0.177} \tag{3}$$

(laminar flow, $20 \leqslant \mathrm{De} \leqslant 2000$, $0.7 \leqslant \mathrm{Pr} \leqslant 175$, $0.0267 \leqslant \delta \leqslant 0.0884$),

$$\mathrm{Nu} = 0.00619\,\mathrm{Re}^{0.92}\mathrm{Pr}^{0.4}(1 + 3.455\delta) \tag{4}$$

(turbulent flow, $5\times10^3 \leqslant \mathrm{Re} \leqslant 10^5$, $0.7 \leqslant \mathrm{Pr} \leqslant 5$, $0.0267 \leqslant \delta \leqslant 0.0884$).